Scripta Materialia 194 (2021) 113624

Contents lists available at ScienceDirect

Scripta Materialia

journal homepage: www.elsevier.com/locate/scriptamat

Dislocation-induced large local polarization inhomogeneity of ferroelectric materials

Ning Li[a], Ruixue Zhu[a], Xiaoxing Cheng[b], Heng-Jui Liu[c], Zhangyuan Zhang[a], Yen-Lin Huang[d], Ying-Hao Chu[d,e], Long-Qing Chen[b], Yuichi Ikuhara[f], Peng Gao[a,g,*]

[a] International Center for Quantum Materials, and Electron Microscopy Laboratory, School of Physics, Peking University, Beijing 100871, China
[b] Department of Materials Science and Engineering, The Pennsylvania State University, University Park, Pennsylvania 16802, USA
[c] Department of Materials Science and Engineering, National Chung Hsing University, Taichung 40227, Taiwan, ROC
[d] Department of Materials Science and Engineering, National Chiao Tung University, Hsinchu 30010, Taiwan, ROC
[e] Institute of Physics, Academia Sinica, Taipei 11529, Taiwan, ROC
[f] Institute of Engineering Innovation, The University of Tokyo, Tokyo 113–8656, Japan
[g] Collaborative Innovation Centre of Quantum Matter, Beijing 100871, China

ARTICLE INFO

Article history:
Received 19 March 2020
Revised 25 October 2020
Accepted 9 November 2020
Available online 27 November 2020

Keywords:
Dislocations
PZT/STO
ferroelectricity
polarization inhomogeneity
STEM

ABSTRACT

Dislocations in ferroelectrics play important roles in ferroelectricity, piezoelectricity, and dielectricity. However, the intrinsic charge-lattice coupling mechanism in ferroelectric crystals containing dislocations is still not well understood. Here, we report a large local polarization inhomogeneity of ~100 μCcm^{-2} induced by a single **a**[001] dislocation in the $PbZr_{0.2}Ti_{0.8}O_3/SrTiO_3$ film/substrate heterostructure, the tensile region (~120 μCcm^{-2}) and the compressive strain region (~21 μCcm^{-2}) around the dislocation forms a butterfly-like area. This study reveals the dramatic effects of dislocations on local polarization and provides a strategy to manipulate the polarization magnitude and orientation of local polarization by defect engineering.

Dislocations are one-dimensional defects that commonly exist in crystalline materials [1]. Such a widely existing defect may alter the chemical composition and stoichiometry of a material, thus drastically influencing certain properties such as low-field magnetoresistance in magnetic films [2], electronic conductors and ionic conductors [3–5], current densities in superconductors [6,7], and spin-polarized current in topological insulators [8]. In ferroelectric materials, due to the intrinsically strong lattice-charge coupling, dislocations play crucial roles in determining the ferroelectric properties. For example, it was reported that the piezoelectric [9] and dielectric responses [10] and phase transition temperatures [9,11,12] are significantly degraded by dislocations due to the formation of a ferroelectric interfacial deadlayers. The influence of dislocations on polarization is not localized, e.g., the interfacial dislocations can alter the polarization magnitude over an extended volume [13]. Even if a dislocation is located in the substrate outside the ferroelectric layer, that dislocation can still interact with the ferroelectric dipoles and suppress the polarization of the ferroelectric layer far away from the interface [14]. Furthermore, the dislocations can interact the domain walls [15] and reduce their mobilities [16–18], as shown by the strong pinning for 90° ferroelastic domain walls [19] and weak pinning for 180° ferroelectric domain walls [20].

In these oxide materials, the effects of dislocations are mainly manifested by the possible nonstoichiometry at these defects and the presence of strain and/or strain gradient. It is generally believed that the electrical activity of dislocations is governed by the elemental segregation and the associated nonstoichiometry around dislocation cores [21,22], which generates the spatial charge zone [23,24]. In fact, in addition to elemental segregation, local strain and strain gradients may play equally important roles in determining electrical activity via piezoelectric and/or flexoelectric effects. In view of the large strain gradient [13] around dislocations, the effect of flexoelectricity on dielectric/ferroelectric materials cannot be ignored [13,25,26]. For example, in a paraelectric $SrTiO_3$ (STO) low-angle bicrystal, an anomalously large polarization of approximately 28 μCcm^{-2} was detected near dislocation cores, which can be attributed to the flexoelectric effect [25]. Additionally, the variable tetragonality near dislocation cores has a crucial influence on polarization [27–30]. Therefore, the influence of a specific dislocation on the polarization in ferroelectric thin films remains unclear.

* Corresponding author.
E-mail address: p-gao@pku.edu.cn (P. Gao).

https://doi.org/10.1016/j.scriptamat.2020.11.009
1359-6462/

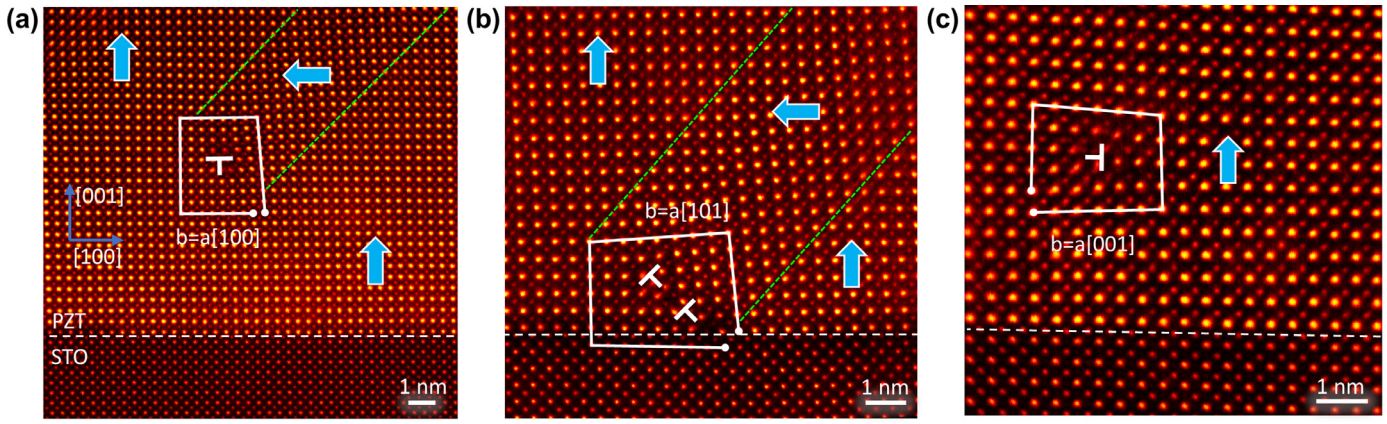

Fig. 1. Atomically resolved high angle annular dark field (HAADF) images of dislocations near the interface. These dislocations are distinguished by the burgers vectors denoted as (a) a[100], (b) a[101], and (c) a[001] respectively. The dislocation cores are labeled by 'T'. Polarization direction is denoted by blue arrows in each figure, the dashed green lines in (a) and (b) denote the 90° domain walls.

The difficulties in studying dislocation effects are mainly associated with the structural characterization at the atomic level and the strong lattice-charge interactions. In addition, dislocations with different Burgers vectors exhibit distinct properties due to their strong structural dependency. For example, in the same perovskite material PZT, dislocations with **a**[100], **a**[110] Burgers vectors [11,19] show extinct properties. Nevertheless, advances in aberration-corrected electron microscopy techniques, especially the negative spherical aberration technique [31], annular bright field (ABF) technique [32,33] and integrated differential phase-contrast (iDPC) technique [34,35], enable direct visualization of all atoms, including oxygen atoms at and near dislocations, allowing us to quantitatively measure the local polarization and strain distributions and revealing the effects of dislocations on polarization. Also, we can easily determine the Burgers vectors of specified dislocations by the atomically resolved images.

Here, we characterize the dislocations in $PbZr_{0.2}Ti_{0.8}O_3$ (PZT) films on an STO substrate using atomically resolved ABF imaging and quantitative image analysis, energy dispersive X-ray spectroscopy (EDS), and phase field simulations. We find that for **a**[001] dislocations, the out-of-plane polarization is notably enhanced up to ~120 $\mu C/cm^2$ in the tensile strain zone over a region of a few nanometers, whereas there is a substantial suppression in polarization of ~21 $\mu C/cm^2$ in the compressive strain region. This large inhomogeneity in polarization around the dislocation can be attributed to the acutely altered tetragonality (strain effect) rather than the flexoelectric effect (strain gradient effect). In contrast, the **a**[101] and **a**[100] dislocations and the triggered in-plane ferroelastic domains induced large strain in PZT and PZT/STO interface separately. Our study precisely correlates the Burges vectors of dislocations with their effects on local polarization, revealing the underlying mechanism, and this study provides a reliable interpretation/prediction of the effects of dislocations in ferroelectric devices (e.g., domain wall pinning). The ability to tune polarization in terms of both orientation and magnitude by controlling the Burgers vectors through introducing different dislocations may also provide strategies to create emergent polar structures, such as a topological polar vortex, an antivortex, and skyrmions.

The atomically resolved high-angle annular dark field (HAADF) of the scanning transmission electron microscopy (STEM) images in Fig. 1 shows three typical dislocations near the interface of the PZT thin films. These dislocations are distinguished by the Burgers vectors denoted as **a**[100], **a**[101], and **a**[001] in Figs. 1(a)-1(c), for which the cores are denoted by a yellow 'T' symbol. The geometric phase analysis for each dislocation in Fig. S1 suggests that the former two are associated with ferroelastic domains that are consistent with previous observations [11,18,36–41]. However, no ferroelastic domain is generated around the dislocation of **a**[001] in Fig. 1(c), indicating that the properties of dislocations are highly dependent on the structure. The structures of the dislocation cores are shown in Fig. S1 in the Supplemental Material.

To reveal the effects of the **a**[001] dislocation on the polarization distribution, we record the corresponding ABF image in Fig. 2(a) from which all the atoms, including the oxygen of PZT, are visible. Once the atoms are accurately positioned, the bond length, lattice constant and polarization are mapped (see Supplemental Material for the detailed calculation method). The substantial inhomogeneity of out-of-plane polarization shows a butterfly shape with enhanced polarization along the two wings. From the bond length mapping of TiO_2 and PbO sublattices in Supplemental Material Fig. S2, both TiO_2 and PbO planes contribute to the polarization enhancement, but the latter has a larger contribution than the former. The profiles in Fig. 2(c) illustrate that the polarization enhancement in the tensile strain zone reaches ~120 μCcm^{-2}, which is 114% greater than that of the local spontaneous polarization (~56 μCcm^{-2}) in the region 8 unit cells away from the core. On the left side of the dislocation core with compressed strain, the polarization is substantially suppressed by 62%. The in-plane component of polarization is also measured in Fig. S3, from which no substantial in-plane polarization is observed, revealing that the trend to form a ferroelastic domain does not occur. Furthermore, there is a bent 180° domain wall across the **a**[001] dislocation, as highlighted by the yellow dashed lines in Fig. 2(b), indicating a possible domain wall pinning effect, which was also reported in previous studies [20,42].

According to the literature, local polarization enhancement can be induced by elemental segregation [3,43–46], strain caused by c lattice changes [14,15,47,48] and strain gradients [25]. To determine the effect of elemental segregation on polarization, we performed EDS analysis. The results in Fig. S4 indicate a uniformly elemental distribution, meaning that there are no significant effects from elemental segregation. In view of the broken translation of symmetry and large deformation of the lattice near the dislocation core, the occurrence of strain and strain gradients is inevitable, and both can considerably influence the polarization. In the mathematica expression, strain can be considered as the 1st deviation of the lattice constant (x'), and the strain gradient is proportional to the 2nd deviation (x''). Based on Landau-Ginzburg-Devonshire (LGD) theory [30],

$$P = \left(\frac{x_3 - 2s_{12}x_m/(s_{11}+s_{12})}{Q_{11} - 2s_{12}Q_{12}/(s_{11}+s_{12})} \right)^{1/2}$$

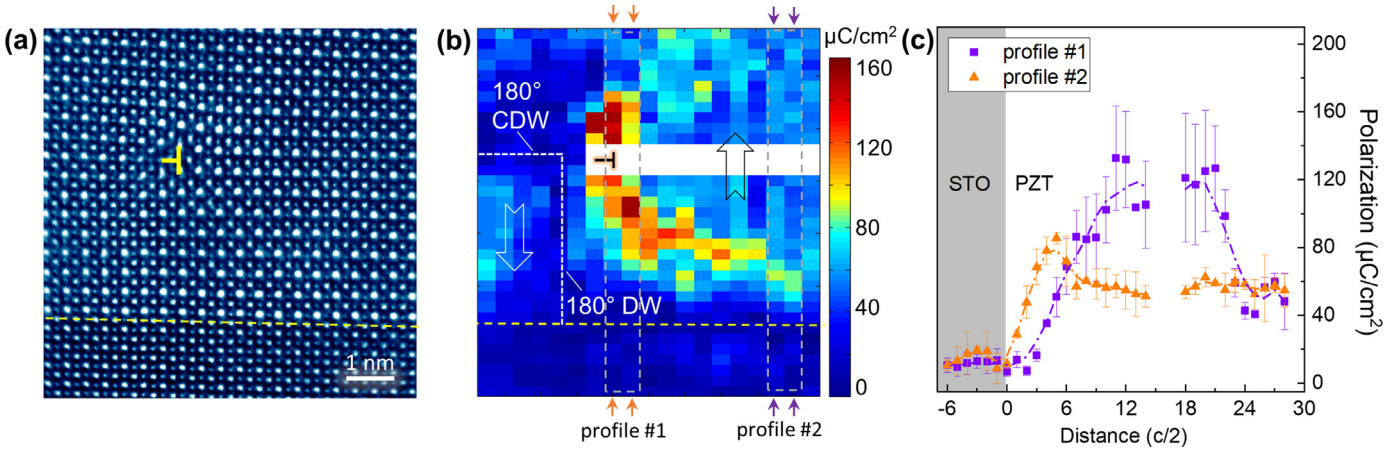

Fig. 2. Quantitative image analysis of a[001] type dislocation. (a) The atomically resolved annular bright field (ABF) image of the same a[001] type dislocation. (b) The calculated polarization at out-of-plane and (c) profiles of out-of-plane polarization at the highlighted region in (b). Two yellow lines in (b) are the 180° charged domain wall and 180° domain wall identified by the Pb-O and Ti-O bond length mapping in Supplemental Material Figure 2.

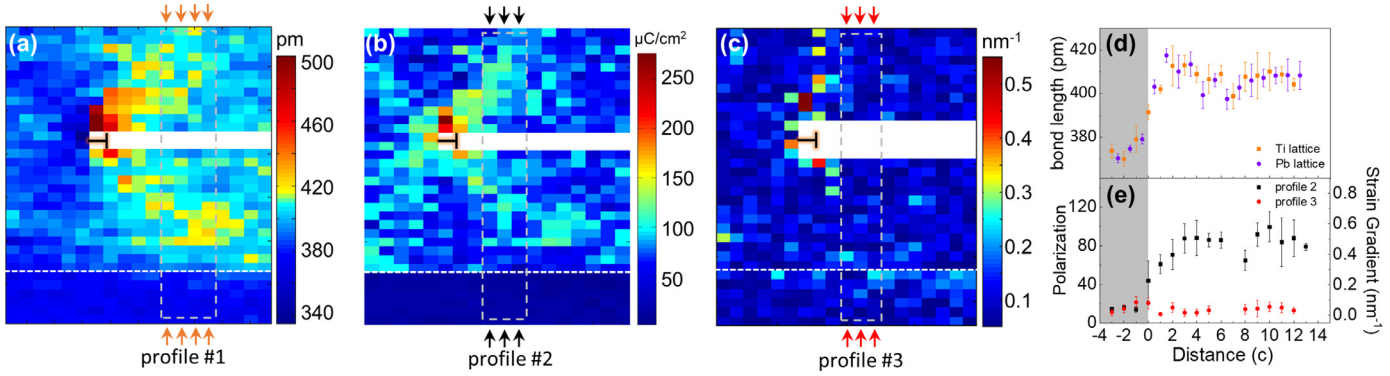

Fig. 3. LGD and flexoelectricity calculations. (a) The map of out-of-plane lattice constant. (b) The calculated polarization from the LGD theory. (c) The calculated strain gradient and flexoelectricity along the out-of-plane direction. The profiles denoted by arrows and dashed gray rectangle in (a-c) are shown in (d) and (e).

where $x_3 = (c - a_p)/a_p$; $x_m = (a - a_p)/a_p$; a and c are in-plane and out-of-plane lattice parameters, respectively; a_p represents the lattice parameter of specified material at room temperature; s_{ij} and Q_{ij} are elastic compliances and electrostrictive coefficients, respectively. In our calculation, a_p is averaged from the a and c data of a uniform region, the other constant values of Q_{ij} and s_{ij} are adopted from [30], and the effect of strain can be quantitatively estimated using the unit-cell level bond length values. Fig. 3(a) displays the out-of-plane lattice constant of both the Pb-Pb and Ti-Ti bonds for comparison. The result calculated from LGD theory in Fig. 3(b) shows that the magnitude distribution has a butterfly shape similar to that of the lattice constant in Fig. 3(a) and the polarization in Fig. 2(b), suggesting that strain may play an important role in polarization enhancement.

The effects of strain gradient, also known as the flexoelectric effect [49], may play important roles in determining the local polarization around the dislocations in oxides because they usually have a large flexoelectric coefficient, and there is a high strain gradient [13] near the cores of dislocations. The out-of-plane strain gradient- and flexoelectric effect-induced polarization mapping is shown in Fig. 3(c). The profiles in Figs. 3(d) and 3(e) show that the flexoelectric effect has a small influence on polarization, and these effects are limited to a size region encompassing two unit cells around a dislocation core, which is substantially different from the significant flexoelectric effect reported for STO [24]. Thus, the flexoelectric effect minimally contributes to the butterfly-like polarization enhancement zones. The above results support the conclusion that strain instead of strain gradient is the main reason for this large enhancement. However, it should also be noted that although the tetragonality in Fig. 3(a) shows the same trend as the polarization distribution in Fig. 2(b), the values calculated from LGD theory are not in quantitative agreement with the polarization, indicating that either the strain effect is not the sole mechanism or the LGD theory cannot precisely describe this system.

To further validate the experimental calculations, we performed a phase field simulation under conditions mimicking the experiments. Due to the lack of trustworthy flexoelectric coupling coefficients for PZT(20/80) in the literature, we choose their values based on our experience from other perovskite dielectric and piezoelectric materials, such as $SrTiO_3$ and $BaTiO_3$ [49], setting f_{11}=1V, f_{12}=1V, and f_{44}=1V for a qualitative comparison. Fig. 4(a) shows the strain-induced out-of-plane polarization around a single **a**[001] dislocation. The polarization is enhanced in the tensile strain region (the right side of the dislocation core) and is reduced in the compressive region. This simulation is in good agreement with the experimental results in Fig. 2(b). In contrast, the strain gradient-induced polarization in Fig. 4(b) is small and has different enhancement and suppression behaviors from those of strain-induced out-of-plane polarization, further confirming that the main factor leading to polarization enhancement is strain rather than the strain gradient. However, it should be noted that the maximum polarization is smaller while the extending region is larger than that of the experimental results. This difference is likely a result of the underestimation of strain-induced structural distortion in the simulation, i.e., the structural distortions are larger near the dislocation cores, and thus, polarization inhomogeneity is

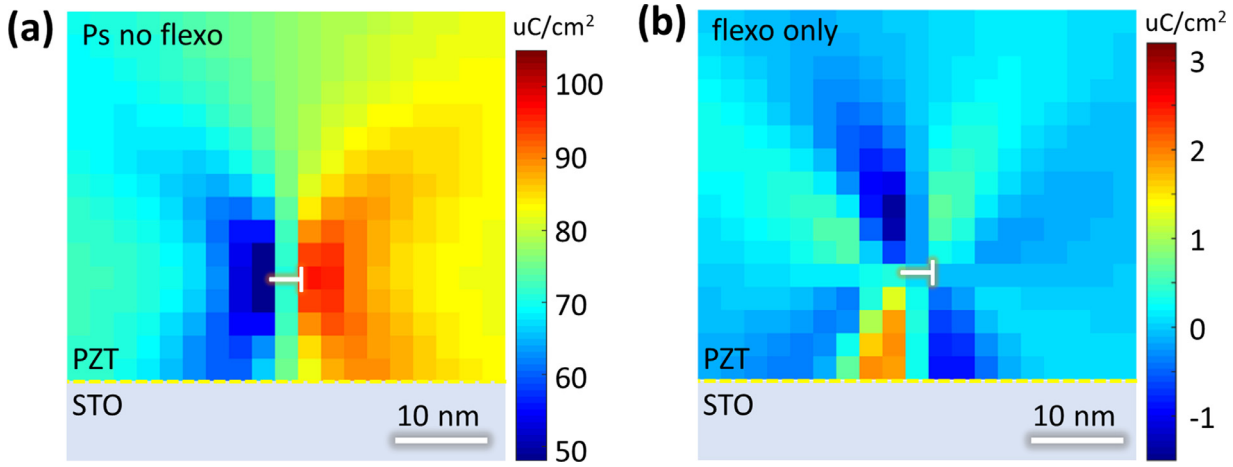

Fig. 4. Phase field simulation. (a) The out of plane polarization without considering the influence of flexoelectric effect and (b) the distribution of the polarization only caused by flexoelectric effect.

expected to be more significant in the experiments than in the simulations.

The dislocation and breaking of the associated translational symmetry greatly affect the ferroelectric material properties; even a single dislocation has many nontrivial influences. The **a**[100] and **a**[101] dislocations commonly exist in the thin film due to the lattice mismatch. But the **a**[001] dislocation are rare to be found, which we surmise it may result from the fluctuation of growth parameters during the growth processes. The highly dependent nature of the physical properties on the structure requires that the properties are correlated to the atomic structure for each dislocation, thus indicating the significance of studying materials from the unit cell level using electron microscopy. Moreover, from the lattice and measured bond length data, a deflected 180° domain wall, which is denoted by a dashed line in Fig. 2(b), can be identified. This finding may elucidate the mechanism of domain wall pinning by dislocations. That is, the compressive strain zone may be more ready to switch due to the suppression of polarization, while the tensile strain zone is more difficult to switch by external fields because of the enhanced polarization, which requires a large amount of bound polarization charges; thus, a larger field is required to drive the domain pass though the dislocation core, leading to domain wall pinning. In fact, the 180° domain wall pinning by dislocations was observed during ferroelectric switching [20].

In summary, we characterized dislocations with different Burgers vectors in the ferroelectric material PZT. Dislocations of **a**[100] and **a**[101] are more likely symbiotic with ferroelastic 90° domain walls [50], while dislocations of **a**[001] cause a strong inhomogeneity of out-of-plane polarization around the dislocation core. By comparing the calculation results of LGD theory and the flexoelectric effect, we find that the local polarization enhancement near this single dislocation is dominated by strain rather than a strain gradient. The mechanism elucidated in our experiment can help us understand the impact of lattice-charge interactions at the atomic scale, thus providing new insights for manipulating local polarization or even creating novel topological polar structures via defect engineering.

Declaration of Competing Interest

The authors declare that they have no known competing financial interests or personal relationships that could have appeared to influence the work reported in this paper.

Acknowledgements

P.G. acknowledges the support from the National Basic Research Program of China (2016YFA0300804), the National Natural Science Foundation of China (51672007, 11974023), and the Key Area R&D Program of Guangdong Province (2018B010109009). The Key R&D Program of Guangdong Province (2018B030327001), the National Equipment Program of China (ZDYZ2015-1), and the “2011 Program” of Peking-Tsinghua-IOP Collaborative Innovation Centre for Quantum Matter. X.X.C. and L.-Q.C were supported by the Computational Materials Sciences Program funded by the US Department of Energy, Office of Science, Basic Energy Sciences, under Award Number DE-SC0020145. H.-J.L. and Y.-H.C. were supported by the Ministry of Science and Technology, R.O.C. (MOST 103-2119-M-009-003-MY3), and the Centre for Interdisciplinary Science of National Chiao Tung University. Part of this study was supported by a Grant-in-Aid for Specially Promoted Research (Grant No. JP17H06094) and a Grant-in-Aid for Scientific Research on Innovative Areas “Nano Informatics” from the Japan Society for the Promotion of Science (JSPS), a Grant-in-Aid for Scientific Research on Innovative Areas “Nano Informatics” (Grant No. 25106003) from JSPS, and the “Nanotechnology Platform” (Project No. 12024046) from the Ministry of Education, Culture, Sports, Science and Technology in Japan (MEXT).

Supplementary materials

Supplementary material associated with this article can be found, in the online version, at doi:10.1016/j.scriptamat.2020.11.009.

References

[1] Y. Ikuhara, Progress in Materials Science 54 (2009) 770–791.
[2] L.B. Steren, M. Sirena, J. Guimpel, Journal of magnetism and magnetic materials 211 (2000) 28–34.
[3] Z. Zhang, W. Sigle, W. Kurtz, M. Rühle, Physical Review B 66 (2002) 214112.
[4] K.K. Adepalli, J. Yang, J. Maier, H.L. Tuller, B. Yildiz, Advanced Functional Materials 27 (2017) 1700243.
[5] L. Lymperakis, J. Neugebauer, M. Albrecht, T. Remmele, H. Strunk, Physical review letters 93 (2004) 196401.
[6] W.W. Webb, Physical review letters 11 (1963) 191–193.
[7] B. Dam, J. Huijbregtse, F. Klaassen, R. Van der Geest, G. Doornbos, J. Rector, A. Testa, S. Freisem, J. Martinez, B. Stäuble-Pümpin, Nature 399 (1999) 439.
[8] Y. Ran, Y. Zhang, A. Vishwanath, Nature Physics 5 (2009) 298.
[9] V. Nagarajan, S. Prasertchoung, T. Zhao, H. Zheng, J. Ouyang, R. Ramesh, W. Tian, X. Pan, D. Kim, C. Eom, Applied Physics Letters 84 (2004) 5225–5227.
[10] C. Canedy, H. Li, S. Alpay, L. Salamanca-Riba, A. Roytburd, R. Ramesh, Applied Physics Letters 77 (2000) 1695–1697.

[11] M.-W. Chu, I. Szafraniak, R. Scholz, C. Harnagea, D. Hesse, M. Alexe, U. Gösele, Nature Materials 3 (2004) 87.
[12] I. Misirlioglu, A. Vasiliev, M. Aindow, S. Alpay, Integrated Ferroelectrics 71 (2005) 67–80.
[13] Y.L. Tang, Y.L. Zhu, Y. Liu, Y.J. Wang, X.L. Ma, Nature Communications 8 (2017) 15994.
[14] C.L. Jia, S.B. Mi, K. Urban, I. Vrejoiu, M. Alexe, D. Hesse, Physical review letters 102 (2009) 117601.
[15] A. Lubk, M.D. Rossell, J. Seidel, Y.H. Chu, R. Ramesh, M.J. Hytch, E. Snoeck, Nano Letters 13 (2013) 1410–1415.
[16] A.Y. Emelyanov, N.A. Pertsev, Physical Review B 68 (2003) 214103.
[17] M.-W. Chu, I. Szafraniak, D. Hesse, M. Alexe, U. Gösele, Physical Review B 72 (2005) 174112.
[18] D. Su, Q. Meng, C. Vaz, M.-G. Han, Y. Segal, F.J. Walker, M. Sawicki, C. Broadbridge, C.H. Ahn, Applied Physics Letters 99 (2011) 102902.
[19] P. Gao, J. Britson, C.T. Nelson, J.R. Jokisaari, C. Duan, M. Trassin, S.H. Baek, H. Guo, L. Li, Y. Wang, Y.H. Chu, A.M. Minor, C.B. Eom, R. Ramesh, L.Q. Chen, X. Pan, Nature Communications 5 (2014) 3801.
[20] P. Gao, C.T. Nelson, J.R. Jokisaari, S.H. Baek, C.W. Bark, Y. Zhang, E. Wang, D.G. Schlom, C.B. Eom, X. Pan, Nature Communications 2 (2011) 591.
[21] Z. Zhang, W. Sigle, M. Rühle, Physical Review B 66 (2002) 094108.
[22] H. Du, C.-L. Jia, L. Houben, V. Metlenko, R.A. De Souza, R. Waser, J. Mayer, Acta materialia 89 (2015) 344–351.
[23] Y.M. Chiang, T. Takagi, Journal of the American Ceramic Society 73 (1990) 3278–3285.
[24] R. Waser, Solid State Ionics 75 (1995) 89–99.
[25] P. Gao, S. Yang, R. Ishikawa, N. Li, B. Feng, A. Kumamoto, N. Shibata, P. Yu, Y. Ikuhara, Physical review letters 120 (2018) 267601.
[26] P. Zubko, G. Catalan, A. Buckley, P.R.L. Welche, J.F. Scott, Physical review letters 99 (2007) 167601.
[27] B.S. Kwak, A. Erbil, B.J. Wilkens, J.D. Budai, M.F. Chisholm, L.A. Boatner, Physical review letters 68 (1992) 3733–3736.
[28] Q.Y. Qiu, V. Nagarajan, S.P. Alpay, Physical Review B 78 (2008) 064117.
[29] B.S. Kwak, A. Erbil, J.D. Budai, M.F. Chisholm, L.A. Boatner, B.J. Wilkens, Phys Rev B Condens Matter 49 (1994) 14865–14879.
[30] D.D. Fong, C. Cionca, Y. Yacoby, G.B. Stephenson, J.A. Eastman, P.H. Fuoss, S.K. Streiffer, C. Thompson, R. Clarke, R. Pindak, E.A. Stern, Physical Review B 71 (2005) 174112.
[31] C. Jia, M. Lentzen, K. Urban, Science 299 (2003) 870–873.
[32] S.D. Findlay, N. Shibata, H. Sawada, E. Okunishi, Y. Kondo, Y. Ikuhara, Ultramicroscopy 110 (2010) 903–923.
[33] P. Gao, R. Ishikawa, B. Feng, A. Kumamoto, N. Shibata, Y. Ikuhara, Ultramicroscopy 184 (2018) 217–224.
[34] I. Lazić, E.G. Bosch, S. Lazar, Ultramicroscopy 160 (2016) 265–280.
[35] E. Yücelen, I. Lazić, E.G. Bosch, Scientific reports 8 (2018) 2676.
[36] S.P. Alpay, I.B. Misirlioglu, V. Nagarajan, R. Ramesh, Applied Physics Letters 85 (2004) 2044–2046.
[37] N. Doukhan, J.C. Doukhan, Physics and Chemistry of Minerals 13 (1986) 403–410.
[38] C.M. Foster, W. Pompe, A.C. Daykin, J.S. Speck, Journal, of Applied Physics 79 (1996) 1405–1415.
[39] H.P. Sun, W. Tian, X.Q. Pan, J.H. Haeni, D.G. Schlom, Applied Physics Letters 84 (2004) 3298–3300.
[40] I. Vrejoiu, G. Le Rhun, N.D. Zakharov, D. Hesse, L. Pintilie, M. Alexe, Philosophical Magazine 86 (2006) 4477–4486.
[41] C.R. Winkler, M.L. Jablonski, K. Ashraf, A.R. Damodaran, K. Jambunathan, J.L. Hart, J.G.G. Wen, D.J. Miller, L.W. Martin, S. Salahuddin, M.L. Taheri, Nano Letters 14 (2014) 3617–3622.
[42] T. Rojac, M. Kosec, B. Budic, N. Setter, D. Damjanovic, Journal of Applied Physics 108 (2010) 074107.
[43] N. Wilcox, V. Ravikumar, R.P. Rodrigues, V.P. Dravid, M. Vollmann, R. Waser, K.K. Soni, A.G. Adriaens, Solid State Ionics 75 (1995) 127–136.
[44] S.Y. Choi, J.P. Buban, M. Nishi, H. Kageyama, N. Shibata, T. Yamamoto, S.J.L. Kang, Y. Ikuhara, Journal of Materials Science 41 (2006) 2621–2625.
[45] J.P. Buban, M.F. Chi, D.J. Masiel, J.P. Bradley, B. Jiang, H. Stahlberg, N.D. Browning, Journal of Materials Research 24 (2009) 2191–2199.
[46] I. Vrejoiu, C. Himcinschi, L. Jin, C.L. Jia, N. Raab, J. Engelmayer, R. Waser, R. Dittmann, P.H.M. van Loosdrecht, Apl Materials 4 (2016) 046103.
[47] X. Li, M. Li, X. Li, S. Tian, A.Y. Abid, N. Li, J. Wang, L. Zhang, X. Li, Y. Zhao, C. Wang, Z. Xu, S. Meng, P. Gao, X. Bai, Acta materialia 170 (2019) 132–137.
[48] L. Li, X. Cheng, J.R. Jokisaari, P. Gao, J. Britson, C. Adamo, C. Heikes, D.G. Schlom, L.Q. Chen, X. Pan, Phys Rev Lett 120 (2018) 137602.
[49] P. Zubko, G. Catalan, A.K. Tagantsev, Annual Review of Materials Research 43 (2013) 387–421.
[50] Y. Liu, Y.L. Tang, Y.L. Zhu, W.Y. Wang, X.L. Ma, Advanced Materials Interfaces 3 (2016).